ELSEVIER

Journal of Power Sources 96 (2001) 151–159

JOURNAL OF POWER SOURCES

www.elsevier.com/locate/jpowsour

Dynamic characterization of small lead-acid cells

Alvin Salkind[a,d,*], Terrill Atwater[a,b], Pritpal Singh[c], Sudarshan Nelatury[c], Sangeetha Damodar[c], Craig Fennie Jr.[e], David Reisner[e]

[a]*Center for Battery Materials & Engineering, Rutgers University, 98 Brett Road, Piscataway, NJ 08854-8058, USA*
[b]*US Army CECOM, RD&EC, Ft. Monmouth, NJ 07703, USA*
[c]*Villanova University, Villanova, PA 19085, USA*
[d]*UMDNJ-Robert Wood Johnson Medical School, Piscataway, NJ 08854, USA*
[e]*US Nanocorp Inc., 74 Batterson Park Road, Farmington, CT 06032, USA*

Received 14 December 2000; accepted 23 December 2000

Abstract

Three sizes of small valve regulated (VRLA) commercially available lead-acid cells were investigated and characterized for their dynamic properties by ac impedance spectroscopy and other electrochemical techniques. All cells were of the limited electrolyte type and no additional electrolyte was introduced during the studies.

The data indicates a very significant increase in cell impedance at lower states of charge, as expected. In charging studies close to the fully charged state, some unexpected impedance data were observed.

Complex impedance plots indicate a passive film formation, probably associated with the recombination surface film. The investigations included cells in various states of charge as well as cycling history including positional orientation studies. Equivalent circuits were derived from ac impedance spectroscopy and the parameters studied as a function of the cell's state-of-charge. Furthermore, the voltage response of the cells was theoretically generated from the ac impedance spectroscopy using Fourier transform analysis and found to be similar to the measured cell responses. © 2001 Published by Elsevier Science B.V.

Keywords: Lead-acid batteries; Electrochemical impedance spectroscopy; Time-domain spectroscopy; Fourier analysis; VRLA batteries

1. Introduction

Performance analysis of lead-acid cells continues to be of technical interest as they are recognized to be rapidly evolving among other successful commercial high power and electric vehicle power sources. The technique of assessing state-of-charge (SOC) based on electrochemical impedance spectroscopy (EIS) [1] is a very popular way to accomplish this. It is also known that for a valid and more thorough dynamic characterization of electrochemical devices, one might reinforce the experimental findings with model parameters derived from relevant mathematical analysis. Further, it is more assuring to have the same inference made from studies made on the basis of two different domains, i.e. both time and frequency.

Time-domain spectroscopy (TDS), which involves the application of a bipolar square wave current and measurement of the consequential terminal voltage, is an emerging technique that attempts to predict the dynamics of cell chemistry by way of quantifying the time constants of the composite exponential response [2]. Be it the case of lead-acid battery, or for that matter any physical system in general, as long as linearity and time-invariance are prevalent, both EIS and TDS are bound to generate the same system–theoretic inference about the underlying processes. It is when these are violated that we find response ambiguities that call for more advanced, nonlinear, analytical methods.

In this paper, we shall show that it is possible to start with EIS data and by subjecting this to a Fourier technique, obtain a TDS response that compares quite well with the measured time domain response. Of particular attention is the distinction between charge and discharge half cycles. We found that during the charge process, the measured TDS almost matches with the Fourier-synthesized response, but during the discharge half-cycle, the predicted results differed from the measured results. To counter this, a small dc voltage bias is employed. This method worked well over the different states of charge considered.

* Corresponding author. Tel.: +1-732-445-6858; fax: +1-732-445-5313.
E-mail address: salkind@rci.rutgers.edu (A. Salkind).

0378-7753/01/$ – see front matter © 2001 Published by Elsevier Science B.V.
PII: S0378-7753(01)00561-4

In addition to ac impedance spectroscopy and time-domain spectroscopy, sweep voltammetry was used to investigate the electrochemical characteristics of the small VRLA lead-acid cells investigated for intermittent high power operations. The cell characteristics of impedance and polarization of these batteries throughout the life of the system were of the most interest and dictated the characterization methods used. To accomplish this, sweep voltammetry and ac impedance spectroscopy were used during both charge and discharge [3,4].

The cell designs of VRLA lead-acid cells investigated included

- a 2.5 Ah, cylindrical spiral wound design R20 (''D'') size [8];
- a 2.0 Ah, flat plate prismatic single cell design [9];
- a 1.0 Ah cylindrical, spiral wound thin film design [10].

In the case of the 2.5 Ah R20 size cell, additional experimentation and modeling was undertaken. Besides impedance spectroscopy, these cells were interrogated with pulsed dc square waves. The 2.0 Ah prismatic and the 1.0 Ah thin film, spiral wound, cylindrical cell was investigated with ac impedance spectroscopy and sweep voltammetry during both charge and discharge.

2. The ac impedance spectroscopy

To study the electrochemical behavior of cells, dc techniques such as cyclic voltammetry, potentiostatic and galvanostatic polarization have been employed. When these techniques are correctly implemented, one might derive a vast amount of information about the kinetic and thermodynamic behavior of the electrodes. But as a variety of complex parallel processes occur at the electrodes, it is hard to elicit the required information. The dc techniques, by themselves, do not provide sufficient information to extract the various kinetic and thermodynamic processes occurring at the electrodes.

Recent literature [5,6] has dealt with deriving several physical models based on the differential equations governing the charge transfer rate and transport of species to the electrolyte/electrode interface. This approach is capable of explaining the occurrence of inductive behavior and negative resistance. Both analytical and numerical methods have been applied to solving these differential equations [5,6]. One useful technique to experimentally confirm the battery models is ac electrochemical impedance spectroscopy. In this method, a small amplitude ac signal (voltage/current) is used as the excitation and the resultant current/voltage response is measured from which the cell's impedance over a range of frequencies is derived. This impedance data is helpful for obtaining the equivalent circuit models for the cell. These models consist of discrete or distributed components. Also one might predict the rate-controlling step in the interfacial Faradaic process.

3. Time-domain spectroscopy

In this technique, a symmetrical, bipolar, square wave current is applied at the terminals of the battery and the consequential voltage is measured. We have developed two different schemes to get the same TDS response. In the first approach, we collect the EIS Data and fit an equivalent circuit model. Analytical expressions are available to get the voltage response due to a given current excitation. In the second approach, we use a Fourier technique to get the TDS response. Results indicate that there is a good match between the measured response and the predicted response.

4. Circuit–theoretical approach

The voltage response of an electrochemical system can be predicted using a purely circuit–theory approach. Equivalent circuits consisting of discrete or distributed components are used in combination to describe an electrochemical system. These circuits include the following subcircuits:

- a resistor in parallel with a capacitor (RC);
- a resistor in parallel with an inductor (RL);
- a constant phase element (CPE);
- a CPE in parallel with a resistor.

The voltage responses of these subcircuits (RC, RL, CPE and CPE in parallel with a resistor) to a step current excitation are shown in Eqs. (1)–(5), respectively. These equations define the temporal voltage response of the circuits for time (t) greater than 0. The total voltage can be found from the sum of the individual contributions.

For the resistor in parallel with a capacitor, the response is given by

$$v(t) = R\left(1 - \exp\left(-\frac{t}{RC}\right)\right) \tag{1}$$

where $v(t)$ is the voltage across the circuit as a function of time, R the parallel resistance, C the parallel capacitance, and t time.

For the resistor in parallel with an inductor, the voltage response is given by

$$v(t) = R\exp\left(-\frac{tR}{L}\right) \tag{2}$$

where L is the parallel inductance. The voltage response of a single CPE element $1/Ts^p$ is given by

$$v(t) = \frac{t^p}{T\Gamma(p+1)} \tag{3}$$

where Γ is the gamma function. The voltage response of a CPE element in parallel with a resistor R is given by

$$v(t) = R\left[\sum_{i=1}^{\infty}(-1)^{i-1}\frac{1}{(RT)^i}\frac{t^{ip}}{\Gamma(ip+1)}\right] \tag{4}$$

A special case when $P = 0.5$ results in a simplification to this equation:

$$v(t) = R\left(1 - \exp\left(\frac{t}{R^2T^2}\right)\operatorname{erfc}\left(\frac{\sqrt{t}}{RT}\right)\right) \quad (5)$$

where erfc is the complementary error function.

The total voltage response derived from Eqs. (1)–(5) is due to a unit current step excitation. The voltage response due to a bipolar square wave current excitation, $V_{\mathrm{bpsw}}(t)$, is then the corresponding sum of time shifted and weighted (± 2) unit step responses as described by Eq. (6):

$$v_{\mathrm{bpsw}}(t) = v_{\mathrm{u}}(t) + 2\sum_{i=1}^{\infty}(-1)^i v_{\mathrm{u}}\left(t - i\frac{T}{2}\right) \quad (6)$$

where $v_{\mathrm{u}}(t)$ is the unit step response and T the period of the square wave excitation.

5. Fourier technique

In order to transform the frequency domain information to the time domain, we would like ideally to acquire the responses at the fundamental frequency and all of the odd harmonics (since the even harmonics are not present in a symmetric square wave). However, since the amplitude of the nth harmonic is $1/n$ times the fundamental, we can window the response up to the 80th harmonic without loss of accuracy.

The Fourier synthesis procedure to derive the time domain voltage response from the measured EIS data is shown in Fig. 1. The measured EIS values at the nth harmonic (Z_n) are multiplied by the windowed Fourier spectral coefficients of the bipolar square wave current (I_n). The resultant is the Fourier coefficients of voltage response (v_n). By adding all the individual contributions the total voltage response, $v(t)$, may be obtained, i.e.

$$v(t) = \sum_{n=-40}^{40} v_n \exp\left(\frac{j(2n-1)\pi t}{T}\right) \quad (7)$$

6. Polarization characterization

The electrochemical characteristics of thin film lead-acid cells were determined, as they are related to intermittent high power operations. Lead-acid cells are one of the primary candidates for a rechargeable component of an electrochemical hybrid system. These battery–battery hybrid systems are designed to provide pulse capability and with improved energy density as compared with standard batteries. The cell characteristics of impedance and polarization of these batteries throughout the discharge life of the system and at non steady-state conditions were of the most interest and dictated the characterization methods used. To accomplish this, sweep voltammetry and impedance spectroscopy were used during both charge and discharge.

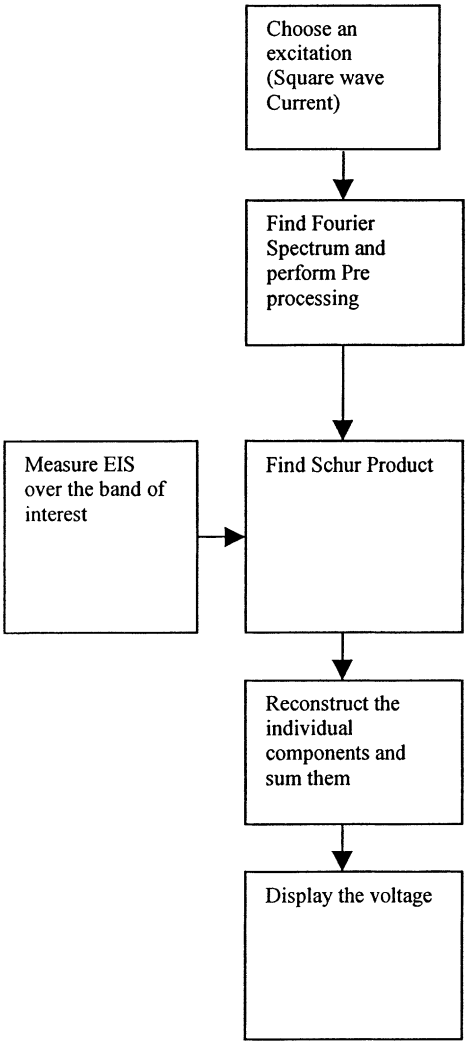

Fig. 1. Flow chart showing Fourier technique for determining a cell's voltage response to a unit step current.

7. Experimental

Impedance data was obtained with a Solartron, SI-1287 Electrochemical Interface and SI-1260 Frequency Response Analyzer controlled by Scribner Associates Inc. CorrWare and Zplot software. The Impedance spectroscopy sweeps were conducted from 65000 to 0.65 Hz at a magnitude of 5 mV. Polarization data was obtained using an Arbin Instruments, Model BT-2043 Automated Battery Test System. The baseline and conditioning current for the cells was set at 200 mA throughout the experiments.

The impedance data on the cylindrical 2.5 Ah cells and some of the time domain data were taken using a Solartron 1280Z combined potentiostat/galvanostat and frequency response analyzer. Additional time domain data was taken with a Solartron 1470 battery analyzer/tester. These

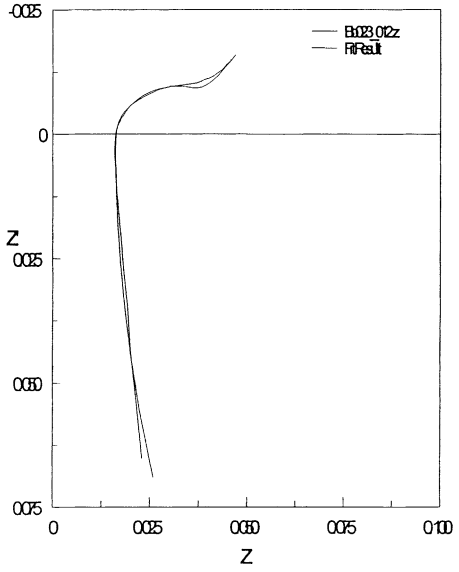

Fig. 2. Electrochemical impedance spectroscopy for a 2.5 Ah, R20 size lead-acid cell at 88% SOC. Real impedance (Z') vs. imaginary impedance (Z'').

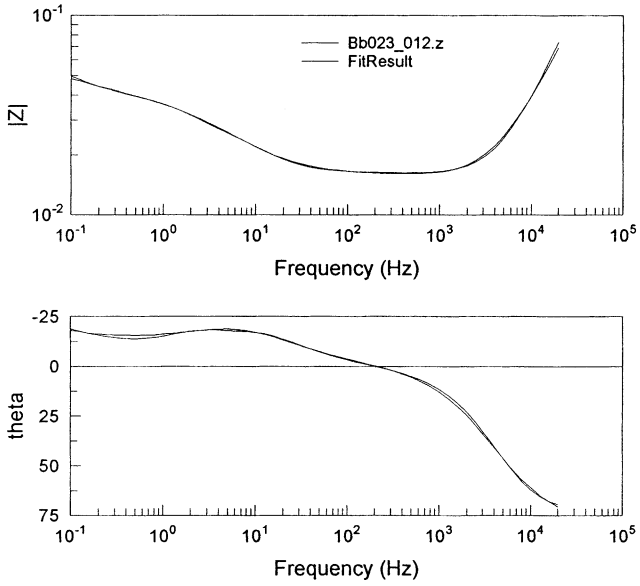

Fig. 3. Electrochemical impedance spectroscopy for a 2.5 Ah, R20 size lead-acid cell at 88% SOC. Magnitude and phase angle vs. frequency.

measurements were made over a frequency range of 0.01 Hz to 10 kHz with an ac amplitude of 10 mV. The time domain measurements were made using a square wave current of ±500 mA and a period of 0.1 Hz.

8. Discussion

Fig. 2 shows a Nyquist plot for a 2.5 Ah, R20 size, cell at 88% SOC and Fig. 3 shows the Bode plots for both the magnitude and phase of the impedance for the same cell and conditions of Fig. 2. The Fourier analysis of the impedance data shown in Figs. 2 and 3 resulted in the time domain response shown dashed in Fig. 4a. Also, Fig. 4a shows the measured time domain response of the cell as a solid line. As can be seen, the time domain response matches up quite well during the charging phase of the bipolar current pulse. However, during the discharging phase, the match is not as good. In order to get a better fit to the measured TDS data,

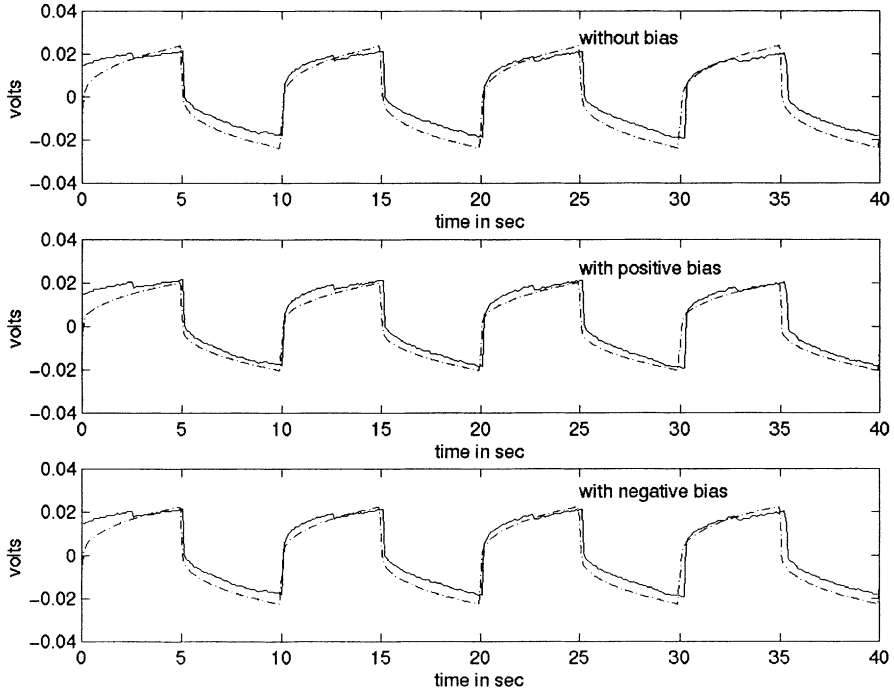

Fig. 4. Voltage response to a bipolar square-wave current obtained through Fourier synthesis technique for a 2.5 Ah, R20 size lead-acid cell. Dashed lines: computed; solid lines: measured results.

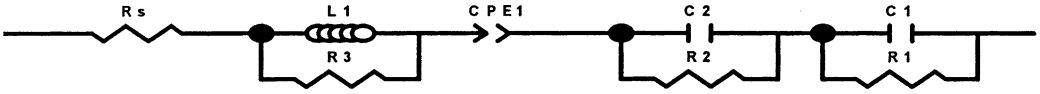

Element	Freedom	Value	Error	Error %
Rs	Free(+)	0.016048	8.6692E-5	0.5402
L1	Free(+)	5.6024E-7	3.6405E-9	0.64981
R3	Free(+)	0.49432	0.039841	8.0598
CPE1-T	Free(+)	60.67	2.9426	4.8502
CPE1-P	Free(+)	0.52469	0.026604	5.0704
C2	Free(+)	7.776	1.0188	13.102
R2	Free(+)	0.010493	0.0008137	7.7547
C1	Free(+)	2.349	0.19445	8.278
R1	Free(+)	0.0062609	0.00068376	10.921

Chi-Squared:	0.0014212
Weighted Sum of Squares:	0.14354
Data File:	D:\aaTds\aEIS_TDS_data\Cell_Bb023\Bb023_012.z
Circuit Model File:	D:\aaTds\aEIS_TDS_data\Zfit\Dd027d.mdl
Mode:	Run Fitting / Selected Points (0 - 54)
Maximum Iterations:	100
Optimization Iterations:	0
Type of Fitting:	Complex
Type of Weighting:	Calc-Modulus

Fig. 5. Electrochemical impedance spectroscopy, equivalent circuit model for a 2.5 Ah, R20 size lead-acid cell.

a voltage bias was added in the analysis. The results of the Fourier analysis with a +10 mV bias added is shown in Fig. 4b (dashed) and with a –10 mV bias added is shown in Fig. 4c (dashed). The figures show that the inclusion of a small, positive bias results in a better fit on the time domain discharge curve whereas a small negative bias results in a worse fit than the zero bias case. This result suggests an inherent nonlinearity in the behavior of the cell as the applied bias is switched from a charging pulse to a discharging pulse.

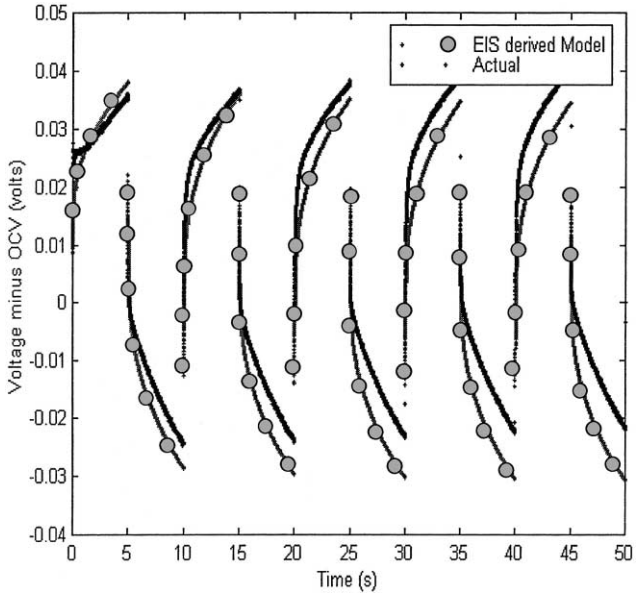

Fig. 6. Bipolar square-wave current for a 2.5 Ah, R20 size lead-acid cell. Voltage response minus open circuit potential.

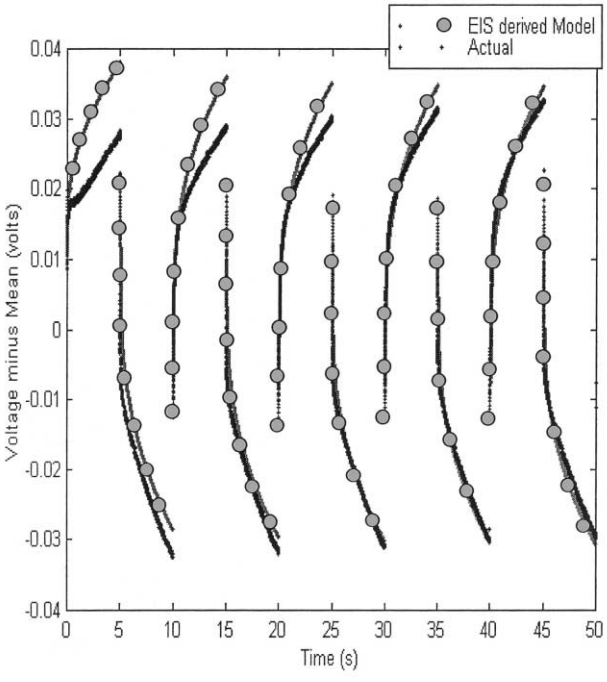

Fig. 7. Bipolar square-wave current for a 2.5 Ah, R20 size lead-acid cell. Voltage response minus mean potential.

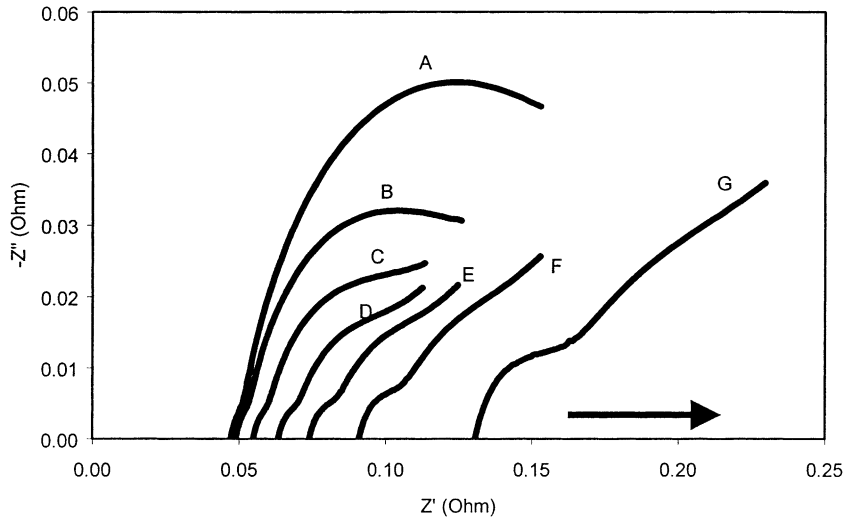

Fig. 8. Electrochemical impedance spectroscopy for a 2.0 Ah prismatic lead-acid cell during discharge cycles. Real impedance (Z') vs. imaginary impedance (Z''). (A) 100% SOC; (B) 83% SOC; (C) 67% SOC; (D) 50% SOC; (E) 33% SOC; (F) 17% SOC; (G) 1% SOC.

The equivalent circuit of the 2.5 Ah cell was derived using Scribner Associates' Zview software. This equivalent circuit, which resulted in an excellent fit to the measured EIS data, comprises an ohmic series resistance, a series inductor in parallel with a resistor, a series CPE element, and two parallel $R-C$ networks. It has been found that the equivalent circuit parameters vary in the anticipated manner with cell SOC. For example, the series resistance, which corresponds to the resistance of the cell's electrolyte increases as the cell SOC decreases. Details of the parametric variation with cell SOC will be reported elsewhere [7].

The time domain response of the cell calculated from the equivalent circuit of Fig. 5 (EIS derived) is shown in Figs. 6 and 7 together with the measured (actual) time domain response of the cell. The curves in Fig. 6 show the measured and the model-predicted cell voltage response curves with the open-circuit voltage of the cells subtracted out, while Fig. 7 shows the corresponding curves with the mean potential subtracted out. Clearly the fit is much better when the voltage response is normalized against the mean potential of the cell. It is also noteworthy that the initial few cycles are of relatively poorer fit compared to later cycles. Furthermore, the discharge curve fit is much better than the charging portion of the cycles confirming the differing behavior of the cell to charging pulses compared to discharging pulses.

The ac impedance spectroscopy data presented in Figs. 8 and 9 show the shift from charge transfer controlled kinetics to diffusion controlled kinetics as the state of charge decreases for the prismatic lead acid cell. The data also shows the expected decrease in the electrolyte conductivity as the sate of charge of the cell decreases. The data presented

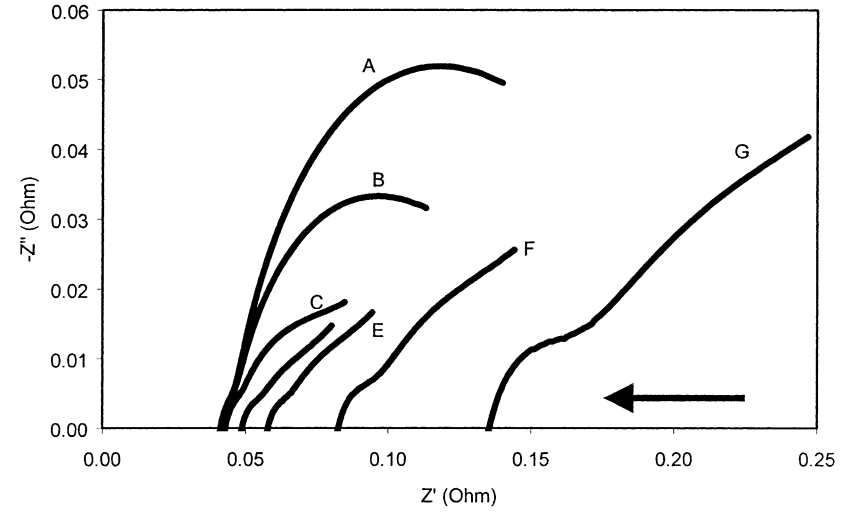

Fig. 9. Electrochemical impedance spectroscopy for a 2.0 Ah prismatic lead-acid cell during charge cycles. Real impedance (Z') vs. imaginary impedance (Z''). (A) 100% SOC; (B) 83% SOC; (C) 67% SOC; (D) 50% SOC; (E) 33% SOC; (F) 17% SOC; (G) 1% SOC.

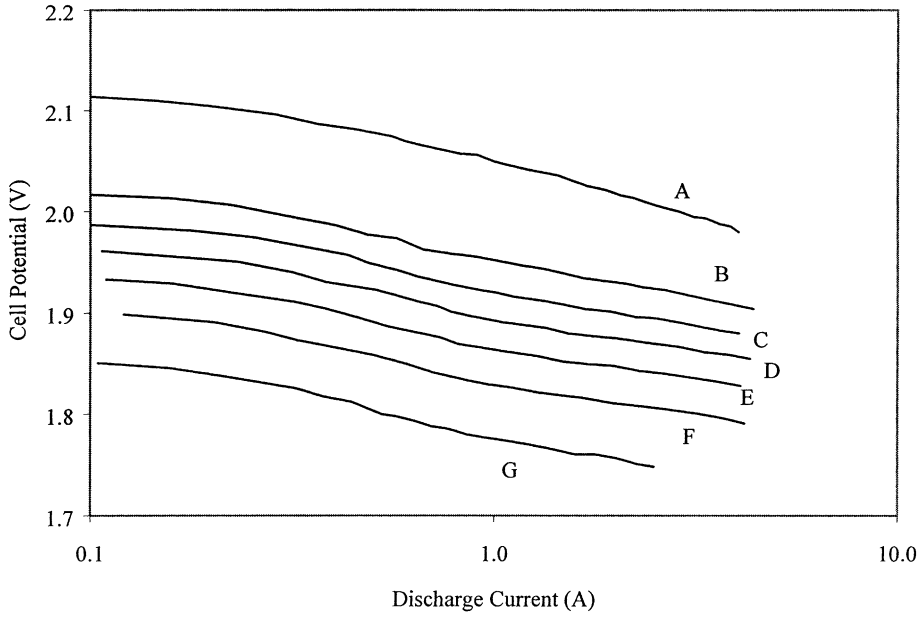

Fig. 10. Discharge polarization characteristics for a 1.0 Ah cylindrical lead-acid cell. (A) 100% SOC; (B) 83% SOC; (C) 67% SOC; (D) 50% SOC; (E) 33% SOC; (F) 17% SOC; (G) 1% SOC.

in Fig. 8 shows the complex impedance for the cell during discharge and Fig. 9 shows the complex impedance for the cell during charge. Comparison of the two sets of data show that at high (100 and 83%) and low (17 and 1%) states-of-charge (SOCs), the complex impedance is comparable. However, for SOCs of 67, 50 and 33%, the data indicates reduced charge transfer for the charging cell compared to the discharging cell while conductivity remains comparable. The data also shows an increase in the complex impedance for the cell at high states of charge. This trend was found to be true for all lead-acid cells tested.

Figs. 10–13 show the discharge and charge polarization for lead-acid cells obtained through sweep voltammetry. A comparison of the discharge characteristics (Figs. 10 and 12) of the cylindrical and prismatic lead-acid cell designs show the greater diffusional limits in the prismatic design during discharge. Figs. 11 and 13 shows that the polarization of both the cylindrical and prismatic cell designs are comparable during charge.

9. Conclusions and future plans

The two commonly utilized techniques of non-invasive interrogation of batteries and other electrochemical devices are impedance spectroscopy and time-domain spectroscopy.

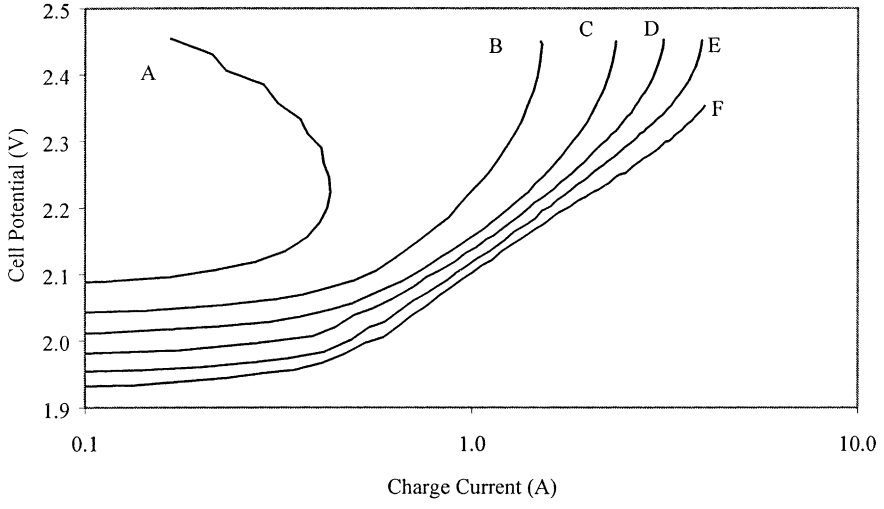

Fig. 11. Charge polarization characteristics for a 1.0 Ah cylindrical lead-acid cell. (A) 100% SOC; (B) 83% SOC; (C) 67% SOC; (D) 50% SOC; (E) 33% SOC; (F) 17% SOC; (G) 1% SOC.

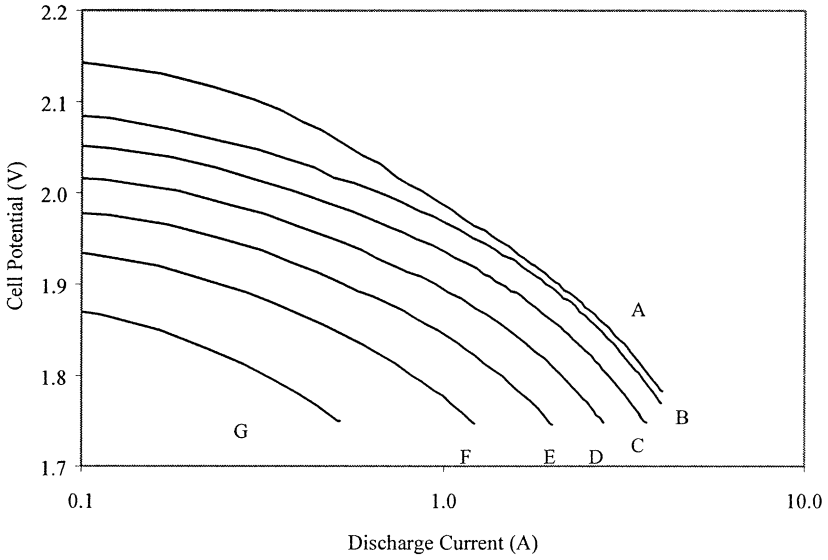

Fig. 12. Discharge polarization characteristics for a 2.0 Ah prismatic lead-acid cell. (A) 100% SOC; (B) 83% SOC; (C) 67% SOC; (D) 50% SOC; (E) 33% SOC; (F) 17% SOC; (G) 1% SOC.

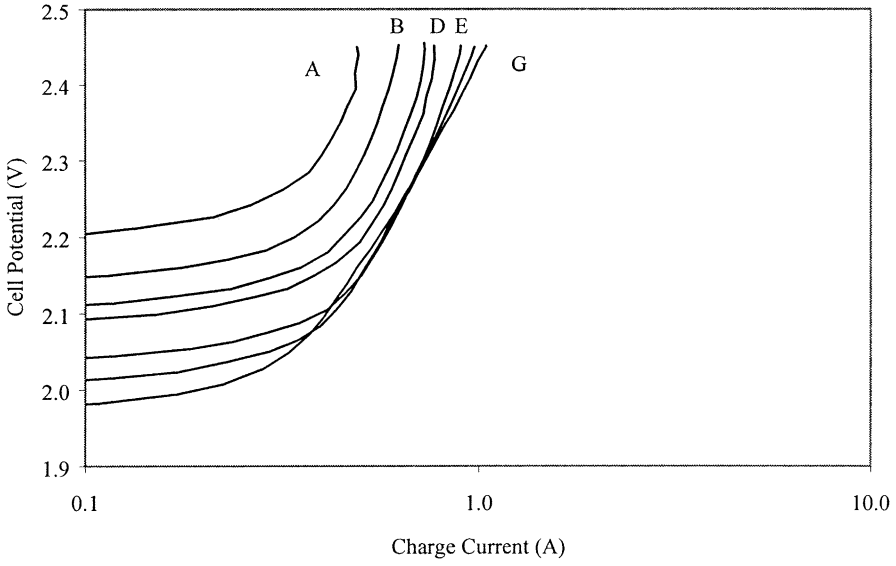

Fig. 13. Charge polarization characteristics for a 2.0 Ah prismatic lead-acid cell. (A) 100% SOC; (B) 83% SOC; (C) 67% SOC; (D) 50% SOC; (E) 33% SOC; (F) 17% SOC; (G) 1% SOC.

In this presentation, they have been shown to relate to the same fundamental properties of electrochemical systems and that the time-domain behavior can be derived from the impedance analysis. Each has some inherent advantages in certain applications, and combined they may provide some distinctive advantages. The data and techniques discussed will enable the fabrication of devices for determination of the SOC of small VRLA cells in the temperature and power range studied.

Other aspects of VRLA cells, for which we plan to seek support for additional studies, include temperature, aging, cycling, and charge techniques factors. In larger cells, there may also be orientation effects.

Acknowledgements

Some of this work was funded through the Southern Coalition for Advanced Transportation under Model no. 35 to ARPA Contract no. MDA972-94-2-0003, dated 13 December 1993.

References

[1] J.R. McDonald, Impedance Spectroscopy, Wiley, New York, 1987.
[2] W. Laletin, Private communication.
[3] T.B. Atwater, L.P. Jarvis, P.J. Cygan, A.J. Salkind, Characteristics of thin film lead-acid cells, in: Proceedings of the 7th ELBC Poster Session and Abstracts, Dublin, Ireland, 19–22 September 2000.

[4] S. Nelatury, S. Damodar, P. Singh, C. Fennie, D. Reisner, A.J. Salkind, A comparative study of time and frequency domain responses of spirally wound lead-acid cells, in: Proceedings of the 7th ELBC Poster Session and Abstracts, Dublin, Ireland, 19–22 September 2000.
[5] J. Newman, W. Tiedemann, AIChE J. 21 (1975) 25.
[6] W.B. Gu, C.Y. Wang, B.Y. Liaw, Numerical modeling of coupled electrochemical and transport processes in lead acid batteries, J. Electrochem. Soc. 144 (6) (1997) 2053–2061.
[7] C. Fennie, S. Nelatury, Y.S. Damodar, P. Singh, D. Reisner, Time and frequency domain modeling of spirally wound lead acid cells, in preparation.
[8] Commercial Product, Hawker North America, 617 N. Ridgeview Dr., Warrensburg, MO 64093-9301, USA.
[9] Commercial Product, Portable Energy Products Inc., 940 Disc Drive, Scotts Valley, CA 95066, USA.
[10] Commercial Product, Bolder Technologies, Corp., 4403 Table Mountain Dr., Golden, CO 80403, USA.